The Interaction of Two Spherical Gas Bubbles in an Infinite Elastic Solid

Florent Chalon, Frank Montheillet

THE INTERACTION OF TWO SPHERICAL GAS BUBBLES IN AN INFINITE ELASTIC SOLID

F. Chalon and F. Montheillet

Division for Materials and Structures Sciences, URA CNRS 1884

Ecole Nationale Supérieure des Mines de Saint-Etienne, France

Abstract

The elastic strain and stress fields between two bubbles of different sizes and different pressures were estimated by using the fundamental result of Eshelby. The equivalent inclusion method was extended to the case of two inclusions in an infinite elastic solid. This approach, which remains totally analytical, was compared successfully to finite element calculations. The mean stress provides information about gas diffusion between the bubbles: according to the results, the bubbles are likely to progressively equalize their sizes. Moreover, the derivation of the von Mises equivalent stress showed that its value, in the vicinity of the bubbles, is larger than the elasticity limit. Therefore, for a complete mechanical description of the problem, plasticity should be taken into account. In spite of its simplicity, this method nevertheless leads to results, which are very close to the prediction of numerical calculations.

Keywords : nuclear fuel, aging, bubbles, stress concentration, equivalent inclusion method.

1. Introduction

The elastic interaction of two spherical cavities with internal pressure (bubbles) is important from the standpoint of materials engineering and has already been investigated by several authors. One of the common applications is the aging of nuclear fuels: nuclear fission produces helium atoms, which form bubbles that eventually damage the material (Lässer [1]). The knowledge of the stress field between two bubbles gives information about their further evolutions. More specifically, the von Mises equivalent stress level is related to the possible occurrence of local damage associated with plastic strain, while the mean stress (hydrostatic pressure) is associated with bubble growth. An analytical or/and numerical approach on this kind of material is necessary, since it is very difficult to carry out direct measurements of the material evolution with time. It is also relevant to derive analytical expressions of the mechanical interaction between two bubbles, that could be simply implemented into more complex numerical models. Sternberg and Sadowsky [2] were the first to be interested in the problem of interaction of two spherical cavities of the same size. They solved it for a uniform field of tension at infinity using the Boussinesq [3] stress-function approach to obtain a series expansion solution. Other authors then extended this method to more than two cavities and for cavities of different sizes under uniaxial loading along the common axis of the cavities, Miyamoto [4], and uniaxial tension in the direction perpendicular to the axis of the cavities, Tsuchida, Nakahara and Kodama [5]. Shelley and Yu [6], still following Sternberg and Sadowsky [2], developed this method for inclusions. Chen and Acrivos [7] extended it to an arbitrary strain field applied at infinity. Willis and Bullough [8] proposed a slightly different approach: they considered the total energy of the bubbles, i.e. the elastic energy, the energy of the gas, and the surface energy. Their approach was therefore not only mechanical but also thermodynamical. They gave a solution for the energy interaction between two excess pressure bubbles but they did not derive precisely the stress field from their results.

All the above authors, except Willis and Bullough, started their analysis with Boussinesq [3], Papkovitch [9] or Neuber [10] functions and gave series expansion solutions. In this work, a different approach is proposed, based on the fundamental result of Eshelby [11] extended to two inhomogeneities. The determination of the eigenstrain of each inclusion from the equivalent inclusion method is used to derive the stress and strain fields between the inclusions. The present approach involving cavities with an internal pressure is the same as for cavities in a material submitted to external loading, but it seems important to explain the transposition from one problem to the other. This method is quite general since it allows the interaction between two gas bubbles of different sizes and different pressures to be investigated. Three configurations are analysed, i.e. two identical bubbles with the same pressure, two bubbles of different sizes with identical pressures and two identical bubbles with different pressures. For each case, the mean stress and von Mises equivalent stress are displayed along the symmetry axis of the bubbles and in the form of iso-value maps. These results are then discussed by comparison with finite element calculations that are described later. It should be noted that, although finite element calculations generally give accurate results for linear problems, they may nevertheless sometimes depart from the exact solution. In particular, finite element solutions around voids are very mesh sensitive. Numerical results need therefore be considered carefully when compared with the analytical derivations.

2. The equivalent inclusion method of Eshelby

Eshelby has established the following fundamental result. Let D be an elastic and isotropic infinite body. Consider Ω as a part of D, small in comparison with D. We can isolate fictitiously Ω which is supposed to represent an ellipsoidal inclusion. Now remove this inclusion from D and impose to it an eigenstrain $\underline{\beta}$, that has no relation with any stress: for example, a thermal deformation or a phase transformation. If the inclusion is replaced into D, which has not been transformed yet, its deformation is no longer free due to the influence of

the surrounding matrix. Thus, a stress field appears in Ω and D. The inclusion deformation, $\underline{\xi}$, due to the presence of the matrix D, is related to the eigenstrain by $\underline{\xi} = \underline{\underline{S}} : \underline{\beta}$, where $\underline{\underline{S}}$ is the fourth order Eshelby tensor. Through this derivation, Eshelby showed that the deformation of an ellipsoidal inclusion embedded in an infinite homogeneous medium, submitted to uniform remote loading, is homogeneous. This result allows the inhomogeneity problem to be dealt with. Consider now an ellipsoidal region, referred to as an inhomogeneity, in an infinite medium, with elastic constants different from the rest of the material.

The Eshelby result is applied to the inhomogeneity. Consider the infinite elastic body of Hooke tensor $\underline{\underline{C}}$, submitted to $\underline{\sigma}^0$ and the corresponding strain $\underline{\varepsilon}^0$ at infinity. The ellipsoidal inhomogeneity Ω with Hooke tensor $\underline{\underline{C}}^i$ disturbs locally the stress field. The aim of the analysis is to determine the perturbations caused by this inhomogeneity. The basic idea of Eshelby is to substitute to the inhomogeneity an homogeneous inclusion with the same properties as the matrix, but submitted to an eigenstrain. The eigenstrain must be determined such as to produce the same stresses and strains as the former inhomogeneity. In the inhomogeneity, the elastic strain is $\underline{\varepsilon}^0 + \underline{\xi}$, whereas in the equivalent inclusion it is given by $\underline{\varepsilon}^0 + \underline{\xi} - \underline{\beta}$. The equivalence condition for the stresses in the inhomogeneity and the inclusion is therefore:

$$\underline{\underline{C}}^i : \left(\underline{\varepsilon}^0 + \underline{\xi}\right) = \underline{\underline{C}} : \left(\underline{\varepsilon}^0 + \underline{\xi} - \underline{\beta}\right) \tag{1}$$

which, combined with $\underline{\xi} = \underline{\underline{S}} : \underline{\beta}$ allows the eigenstrain tensor $\underline{\beta}$ to be determined.

3. Extension of the equivalent inclusion method of Eshelby

While the problem of interacting inhomogeneities cannot be solved in closed form (the "exact" solution involves infinite series expansions [12]), an approximate analytical derivation is proposed below. In a first step, the interaction of two bubbles with equal internal pressures

will be dealt with. Using the superposition principle illustrated in Fig. 1 (a), (b), and (c), it is sufficient to consider merely cavities. Application of the equivalent inclusion method extended to two inclusions then leads accordingly to introduce two eigenstrains, $\underline{\beta}^{I}$ and $\underline{\beta}^{II}$, that depend on the space coordinates. For the sake of simplicity, they will be approximated by their values at the centers of the respective bubbles. In a second step, the effect of a pressure difference Δp between the two bubbles will be addressed in the form of a small perturbation to the above solution. It is worth to note that the boundary conditions at the bubble surfaces, i.e. $\sigma_{rr} = -p$ and $\sigma_{r\theta} = 0$, are not strictly fulfilled by such an estimation of the exact solution.

Solid inhomogeneities will first be considered, but in further derivations their elastic constants will be set equal to zero in order to deal with cavities. The problem, which is axisymmetric, will be solved in a plane containing the centre of the two inhomogeneities. In Fig. 1, the transition from gas bubbles to cavities without internal pressure is shown, with p_1 greater than p_2, $p = (p_1 + p_2)/2$ and $\Delta p = p_1 - p$. The case illustrated in Fig. 1 (b) is more difficult to solve than the other ones that are quite obvious. It seems important to remind that the applied stress at infinity is hydrostatic, so that $\underline{\sigma}^{0}$ is a diagonal tensor.

Problem (b) of Fig. 1 will first be solved for inhomogeneities. Consider two ellipsoidal inhomogeneities Ω_1 and Ω_2 with Hooke tensors $\underline{\underline{C}}^{I}$ and $\underline{\underline{C}}^{II}$ in a matrix with Hooke tensor $\underline{\underline{C}}$ under remote stress $\underline{\sigma}^{0}$. Deformation in inhomogeneity I is influenced by inhomogeneity II such that:

$$\underline{\varepsilon}^{I} = \underline{\varepsilon}^{0} + \underline{\xi}^{I} + \underline{\eta}^{II} \tag{2}$$

with

$$\underline{\xi}^{I} = \underline{\underline{S}} : \underline{\beta}^{I} \tag{3}$$

where $\underline{\underline{S}}$ is constant and the same for the two inclusions since its expression depends only on the shape of the inclusions, which are both spherical here,

and $$\underline{\eta}^{II} = \underline{\underline{D}}^{II} : \underline{\beta}^{II} \tag{4}$$

where $\underline{\underline{D}}^{II}$ is the influence tensor associated with inclusion II. Thus, the strain $\underline{\eta}^{II}$ represents the influence of inclusion II on inclusion I. In the same way, the influence of inclusion I on inclusion II is $\underline{\eta}^{I}$.

Note that the eigenstrains could be expanded in polynomial series, e.g.

$$\beta_{ij}^{II}(\mathbf{x}) = B_{ij}^{II} + B_{ijk}^{II} x_k + B_{ijkl}^{II} x_k x_l + ... \tag{5}$$

As $\underline{\xi} = \underline{\underline{S}} : \underline{\beta}$ and $\underline{\eta} = \underline{\underline{D}} : \underline{\beta}$, they could be expanded in polynomial series in the same way.

However, to a first approximation, the eigenstrains $\underline{\beta}^{I}$ and $\underline{\beta}^{II}$ will be assumed uniform, whence:

$$\underline{\xi}^{I} = \underline{\underline{S}} : \underline{\beta}^{I} \tag{6}$$

is constant while

$$\eta_{ij}^{II}(\mathbf{x}) = D_{ijkl}^{II}(\mathbf{x}) B_{kl}^{II} \tag{7}$$

remains a function of the space variables through the influence tensor.

The equivalence conditions for the stresses in the two inhomogeneities and the two inclusions can now be written:

$$\begin{cases} \underline{\underline{C}}^{I} : \left(\underline{\varepsilon}^{0} + \underline{\xi}^{I} + \underline{\eta}^{II}\right) = \underline{\underline{C}} : \left(\underline{\varepsilon}^{0} + \underline{\xi}^{I} + \underline{\eta}^{II} - \underline{\beta}^{I}\right) & \text{in } \Omega_1 \\ \underline{\underline{C}}^{II} : \left(\underline{\varepsilon}^{0} + \underline{\xi}^{II} + \underline{\eta}^{I}\right) = \underline{\underline{C}} : \left(\underline{\varepsilon}^{0} + \underline{\xi}^{II} + \underline{\eta}^{I} - \underline{\beta}^{II}\right) & \text{in } \Omega_2 \end{cases} \tag{8}$$

Since the material is isotropic, the constitutive equation can be written in the following form:

$$\sigma_{ij} = 2\mu\varepsilon_{ij} + \left(\kappa - 2\mu/3\right)\varepsilon_{kk}\delta_{ij} \tag{9}$$

where κ and μ are the bulk and shear moduli, respectively.

Equation (8) then becomes:

$$
\begin{aligned}
&2\mu^{I}\left(\varepsilon^{0}_{ij}+S_{ijkl}\beta^{I}_{kl}+D^{II}_{ijkl}\beta^{II}_{kl}\right)+\left(\kappa^{I}-2\mu^{I}/3\right)\left(\varepsilon^{0}_{kk}+S_{kkmn}\beta^{I}_{mn}+D^{II}_{kkmn}\beta^{II}_{mn}\right)\delta_{ij}\\
&=2\mu\left(\varepsilon^{0}_{ij}+S_{ijkl}\beta^{I}_{kl}+D^{II}_{ijkl}\beta^{II}_{kl}-\beta^{I}_{ij}\right)+\left(\kappa-2\mu/3\right)\left(\varepsilon^{0}_{kk}+S_{kkmn}\beta^{I}_{mn}+D^{II}_{kkmn}\beta^{II}_{mn}-\beta^{I}_{kk}\right)\delta_{ij} \qquad \text{in } \Omega_1\\
&2\mu^{II}\left(\varepsilon^{0}_{ij}+S_{ijkl}\beta^{II}_{kl}+D^{I}_{ijkl}\beta^{I}_{kl}\right)+\left(\kappa^{II}-2\mu^{II}/3\right)\left(\varepsilon^{0}_{kk}+S_{kkmn}\beta^{II}_{mn}+D^{I}_{kkmn}\beta^{I}_{mn}\right)\delta_{ij}\\
&=2\mu\left(\varepsilon^{0}_{ij}+S_{ijkl}\beta^{II}_{kl}+D^{I}_{ijkl}\beta^{I}_{kl}-\beta^{II}_{ij}\right)+\left(\kappa-2\mu/3\right)\left(\varepsilon^{0}_{kk}+S_{kkmn}\beta^{II}_{mn}+D^{I}_{kkmn}\beta^{I}_{mn}-\beta^{II}_{kk}\right)\delta_{ij} \qquad \text{in } \Omega_2
\end{aligned}
\tag{10}
$$

As seen above, the Eshelby tensors are the same for Ω_1 and Ω_2. The above system must now be solved in order to determine the eigenstrains for each inclusion.

4. Analytical resolution

4.1. Derivation of the influence tensors D_{ijkl}

The expression of D_{ijkl} for a spherical inclusion of radius a is given by Mura [12]:

$$
8\pi(1-\nu)D_{ijkl}(\mathbf{x})=\Psi_{,klij}-2\nu\delta_{kl}\Phi_{,ij}-(1-\nu)\left[\Phi_{,kl}\,\delta_{il}+\Phi_{,ki}\,\delta_{jl}+\Phi_{,lj}\,\delta_{ik}+\Phi_{,li}\,\delta_{jk}\right] \tag{11}
$$

$$
\text{with } \Phi=\frac{1}{2}\left[I(\lambda)-x_k x_k I_K(\lambda)\right] \text{ and } \Psi_{,i}=\frac{x_i}{2}\left[I(\lambda)-x_k x_k I_K(\lambda)-a^2\left(I_I(\lambda)-x_k x_k I_{IK}(\lambda)\right)\right] \tag{12}
$$

$$
\text{and} \qquad \lambda=x_1^2+x_2^2+x_3^2-a^2, \text{ and } I_{\underbrace{IK}_{n}}(\lambda)=\frac{4\pi a^3}{(2n+1)(a^2+\lambda)^{n+1/2}} \tag{13}
$$

Here, the following convention is used: summation from 1 to 3 is extended over repeated lower case indices; capital indices take the same values as the corresponding lower case ones but without summation. Note that, in equation (13), the number of indices n=0, 1 or 2.

As seen before, the unknown eigenstrain tensors $\underline{\beta}^{I}$ and $\underline{\beta}^{II}$ are assumed to be uniform in each inclusion. Owing to axisymmetry, the expressions of the eigenstrains can be simplified (Fig. 2):

Since $\beta_{11}=\beta_{22}$, $\beta_{13}=\beta_{23}$ and $\beta_{12}=0$, only three eigenstrain components are to be determined, namely β_{11}, β_{33} and β_{13}. The linear system (10) then decomposes into one set of four equations for the "diagonal" unknowns β^{I}_{11}, β^{I}_{33}, β^{II}_{11}, and β^{II}_{33} on the one hand, and a set of two

equations for the "non-diagonal" unknowns β_{13}^{I} and β_{13}^{II}. This system will be solved for two inclusions centered at (0,0,0) and (0,0,d). The (constant) values of the two eigenstrain tensors are those derived at the center of the associated inclusion, although such a choice is somewhat arbitrary since they could be calculated anywhere in the inclusions. The derivation is detailed below for one inclusion, Ω_1. Thus, owing to axisymmetry, $\underline{\eta}$ can be written in the following form:

$$\underline{\eta} = \begin{pmatrix} \eta_{11} & 0 & \eta_{13} \\ 0 & \eta_{11} & \eta_{13} \\ \eta_{13} & \eta_{13} & \eta_{33} \end{pmatrix} \tag{14}$$

Therefore only 3x6=18 D_{ijkl} components are needed:

$$D_{1111} = D_{2222} = \frac{9\alpha_2^5 + 5\alpha_2^3(1-2\nu)}{30(1-\nu)} \qquad D_{3333} = \frac{15\alpha_2^5 - 10\alpha_2^3(2-\nu)}{15(1-\nu)}$$

$$D_{1122} = D_{2211} = \frac{3\alpha_2^5 - 5\alpha_2^3(1-2\nu)}{30(1-\nu)} \qquad D_{3311} = D_{3322} = \frac{-6\alpha_2^5 + 5\alpha_2^3(1-2\nu)}{15(1-\nu)}$$

$$D_{1133} = D_{2233} = \frac{-6\alpha_2^5 + 5\alpha_2^3(1+\nu)}{15(1-\nu)} \qquad D_{1313} = D_{2323} = \frac{-12\alpha_2^5 + 5\alpha_2^3(1+\nu)}{30(1-\nu)}$$

and all the other D_{ijkl}=0.

In the above equations, $\alpha_2=a_2/d$, and for the second inclusion the corresponding components are the same with $\alpha_1=a_1/d$.

4.2. Derivation of the eigenstrains and the stress field

As seen above, $\underline{\xi}$ can be written in the following form:

$$\underline{\xi} = \begin{pmatrix} \xi_{11} & 0 & \xi_{13} \\ 0 & \xi_{11} & \xi_{13} \\ \xi_{13} & \xi_{13} & \xi_{33} \end{pmatrix} \tag{15}$$

with the18 associated S_{ijkl}:

$S_{1111}= S_{2222}= S_{3333}=\dfrac{7-5\nu}{15(1-\nu)}$ $\qquad$ $S_{1212}= S_{2323}= S_{3131}=\dfrac{4-5\nu}{15(1-\nu)}$

$S_{1122}= S_{2233}= S_{3311}= S_{1133}= S_{2211}= S_{3322}=\dfrac{5\nu-1}{15(1-\nu)}$ $\qquad$ and all the other $S_{ijkl}=0$.

The system (10) can now be solved. For i and j=1,3, it leads very easily to:

$$\beta_{13}^{I} = \beta_{13}^{II} = 0 \tag{16}$$

so that the system reduces to four equations for only four unknowns. The elastic moduli μ^I, μ^{II}, κ^I and κ^{II} are now set equal to zero, since cavities are considered, and the hydrostatic loading is accounted for by specifying $\varepsilon_{ij}^0=(p/3\kappa)\delta_{ij}$. The following system is obtained:

$$\begin{cases} A_{11}\beta_{11}^{I} + A_{12}\beta_{33}^{I} + A_{13}\beta_{11}^{II} + A_{14}\beta_{33}^{II} = -p \\ A_{21}\beta_{11}^{I} + A_{22}\beta_{33}^{I} + A_{23}\beta_{11}^{II} + A_{24}\beta_{33}^{II} = -p \\ A_{31}\beta_{11}^{I} + A_{32}\beta_{33}^{I} + A_{33}\beta_{11}^{II} + A_{34}\beta_{33}^{II} = -p \\ A_{41}\beta_{11}^{I} + A_{42}\beta_{33}^{I} + A_{43}\beta_{11}^{II} + A_{44}\beta_{33}^{II} = -p \end{cases} \tag{17}$$

where the coefficients A_{ij}, given in the Appendix, depend on the components of the Eshelby and influence tensors. Once the eigenstrains are determined (see Appendix), the interaction fields between the inclusions can be calculated with the help of the influence tensors $\underline{\underline{\underline{\underline{D}}}}^{I}$ and $\underline{\underline{\underline{\underline{D}}}}^{II}$.

The strain field in the matrix associated with the case of Fig. 1 (b) can now been written in the form:

$$\underline{\varepsilon} = \underline{\varepsilon}^{0} + \underline{\underline{\underline{\underline{D}}}}^{I}(x_1, x_2, x_3) : \underline{\beta}^{I} + \underline{\underline{\underline{\underline{D}}}}^{II}(x_1, x_2, x_3) : \underline{\beta}^{II} \tag{18}$$

Owing to the axisymmetric configuration, the interactions are analyzed in the plane (x_1,x_3). Since the eigenstrain tensor has the following diagonal form:

$$\begin{pmatrix} \beta_{11} & 0 & 0 \\ 0 & \beta_{11} & 0 \\ 0 & 0 & \beta_{33} \end{pmatrix} \tag{19}$$

the only required components of the influence tensor are D_{ij11} and D_{ij33}. The interaction strains for the case of Fig. 1 (b) are given by:

$$\eta_{11} = \left(D^{I}_{1111} + D^{I}_{1122}\right)\beta^{I}_{11} + D^{I}_{1133}\beta^{I}_{33} + \left(D^{II}_{1111} + D^{II}_{1122}\right)\beta^{II}_{11} + D^{II}_{1133}\beta^{II}_{33}$$

$$\eta_{22} = \eta_{11} \tag{20}$$

$$\eta_{33} = \left(D^{I}_{3311} + D^{I}_{3322}\right)\beta^{I}_{11} + D^{I}_{3333}\beta^{I}_{33} + \left(D^{II}_{3311} + D^{II}_{3322}\right)\beta^{II}_{11} + D^{II}_{3333}\beta^{II}_{33}$$

Therefore, only 12 components of the influence tensor need be calculated. The stresses for the case of two cavities with the same pressure p are then obtained from the constitutive equation (9). Furthermore, the effect of a pressure difference between the two bubbles may be estimated to a first approximation by adding the stresses determined in (25) below.

It is worth to note that the general solution of the problem proposed here is only an estimation. Indeed we first assumed the eigenstrains uniform. The second approximation is related to the boundary conditions. In order to apply the principle of linear superposition, the tangential components due to the pressure difference between the bubbles are neglected. Under such approximation, the equality between the boundary conditions illustrated in Fig. 1 remains correct.

For two cavities with the same internal pressure p, the solution of the case depicted in Fig. 1 (c) is:

$$\varepsilon^{c0}_{ij} = (-p/3\kappa)\delta_{ij} \tag{21}$$

Since $\varepsilon^{c0}_{ij} + \varepsilon^{0}_{ij} = 0$, the strain field for two interacting cavities with the same pressure is the linear superposition of solutions for the problems illustrated in Fig. 1 (b) and 1 (c):

$$\underline{\varepsilon} = \underline{\underline{D}}^{I}(x_1, x_2, x_3) : \underline{\beta}^{I} + \underline{\underline{D}}^{II}(x_1, x_2, x_3) : \underline{\beta}^{II} \tag{22}$$

The case depicted in Fig. 1 (d) is easy to analyse since the stress field of an isolated bubble in an infinite elastic solid has an analytical expression. If an internal pressure Δp is applied in the absence of remote loading, the displacement field exhibits spherical symmetry:

$$\mathbf{u} = u_r(r)\,\mathbf{e_r} \tag{23}$$

where $\mathbf{e_r}$ denotes the radial unit vector.

Resolution of the equilibrium equations then yields:

$$u(r) = \frac{\Delta p}{4\mu}\frac{a^3}{r^2}, \quad \varepsilon_{rr} = -\frac{\Delta p}{2\mu}\frac{a^3}{r^3}, \quad \varepsilon_{\theta\theta} = \varepsilon_{\varphi\varphi} = \frac{\Delta p}{4\mu}\frac{a^3}{r^3}, \tag{24}$$

$$\sigma_{rr} = -\Delta p\frac{a^3}{r^3}, \quad \sigma_{\theta\theta} = \sigma_{\varphi\varphi} = \frac{\Delta p}{2}\frac{a^3}{r^3} \tag{25}$$

Finally the mean stress and the von Mises equivalent stress are derived:

$$\sigma_m = \frac{1}{3}(\sigma_{11} + \sigma_{22} + \sigma_{33}) \tag{26}$$

$$\bar{\sigma}_{VM} = \sqrt{\frac{1}{2}\left[(\sigma_{11} - \sigma_{22})^2 + (\sigma_{22} - \sigma_{33})^2 + (\sigma_{33} - \sigma_{11})^2\right] + 3(\sigma_{12}^2 + \sigma_{23}^2 + \sigma_{31}^2)} \tag{27}$$

Hence the distribution of the two above quantities for two cavities of different sizes with different pressures can be analyzed.

For the spherical coordinates, we change $1 \rightarrow r$, $2 \rightarrow \theta$, and $3 \rightarrow \varphi$.

5. Results and discussion

It is important to note that for an isolated bubble, the mean stress vanishes at any point:

$$\sigma_{rr} = -\Delta p\frac{a^3}{r^3}, \quad \sigma_{\theta\theta} = \sigma_{\varphi\varphi} = \frac{\Delta p}{2}\frac{a^3}{r^3} \quad \Rightarrow \quad \sigma_m = 0 \tag{28}$$

It is therefore not possible to determine the influence of Δp on the mean stress around the two bubbles because the contribution of the configuration illustrated in Fig. 1 (d) is zero. The above approach is expected, however, to give a good estimation of the von Mises equivalent stress.

The present method allows various configurations to be easily investigated. Three parameters can be changed: the size and pressure of each bubble, and the distance between the bubble centers. In the following, three different cases are considered. The first case (i) consists of two bubbles of same size with same internal pressure, the second one (ii) of two different bubbles of different sizes with same pressure, and the third one (iii) of two bubbles of same size with different pressures. In the two first cases the mean stress and the von Mises equivalent stress are analyzed, while for the third case only the von Mises equivalent stress can be discussed (see above). Two representations of the results are used for each case: the stresses are displayed both along the symmetry axis and on a map in the half plane (x_1,x_3). To discuss the analytical approach, the results are compared with numerical calculations carried out with the Abaqus® software. An example of the mesh used for two bubbles of equal size is given in Fig. 3. It is divided into two different regions: in the first one, close to the cavities, where the stress fields are to be determined precisely, the elements are small. The second one, far away from the cavities, is made of larger elements. To obtain the best results, the mesh must be very fine and the elements must be close to squares. Moreover, for ensuring a good representation of an infinite solid, the mesh is very large compared to the bubble sizes and infinite elements are used far away from the bubbles. These requirements are fulfilled in the mesh. In Fig. 4, the stress distributions along the symmetry axis are displayed for the two first cases. The corresponding maps are given in Fig. 5 and 6. The last case is shown in Fig. 7. All calculations were carried out using the elastic constants of palladium, which is usually employed to store nuclear fuels, i.e. κ=171.3 GPa, μ=42.7 GPa, and ν=0.385.

As shown on the curves and the maps, there are slight differences between the analytical and numerical values of the mean stress, which are very small with respect to the von Mises equivalent stress. This is because the nonzero mean stress is induced by the interaction of the bubbles (it vanishes for an isolated bubble), whereas this interaction only introduces a perturbation of the von Mises equivalent stress.

The errors brought to the exact solution by the above-mentioned approximations can be estimated by considering the values of the normal stresses at the bubble surfaces, in particular along the symmetry axis x_3. The discrepancies between the exact values (i.e., $\sigma_{rr} = -p$) and that predicted by the analytical approach are less than 1% for the three investigated configurations. The largest errors (overestimations) occur of course at points where the two bubbles are facing. Moreover, the gap is significantly smaller along the equators of the bubbles.

In Fig. 4, it is apparent that the analytical curves are very close to the numerical results except for a few points where the latter are slightly larger than the analytical predictions. The assumption of uniform eigenstrains is likely to be responsible for this discrepancy. Similarly, the von Mises equivalent stresses derived analytically (see Fig. 5 and 6), exhibit local maxima along the x_1 and x_3 axes, that can be related to the Taylor first order expansions. This first analysis therefore shows that, despite its simplifying assumptions, the present approach leads to analytical results which are quite similar to the finite element predictions.

The mean stress maps allow the material regions undergoing tensile or compressive loading to be easily localized. Such results can be taken into account in a diffusion model. Helium atoms, after being created by tritium decay, diffuse in the material towards the bubbles. From the point of view of mechanics, the evolution of a pair of bubbles of different sizes can be predicted from the mean stress map in Fig. 6. The tension mean stress is larger near the smaller bubble than near the larger one. Helium atoms will therefore diffuse preferentially towards the small bubble, until the latter reaches the same size as the larger one. It is thus likely that the bubbles will tend to progressively equalize their sizes. This is a part of the mechanism of diffusion, which should be added to a thermodynamical analysis to obtain a complete description of the evolution of the system.

The above results can also be used to predict the occurrence of cracks in the vicinity of the bubbles. The levels of the von Mises equivalent stresses also give quite an important

information about the areas where plasticity occurs, i.e. at each point where the von Mises equivalent stress is larger than the yield stress (0.23 GPa) of the material. Therefore, a complete mechanical description of the material evolution will require to take plasticity into account.

6. Conclusions

A new approach for the estimation of the elastic fields between two bubbles loaded by an internal pressure was proposed. In spite of its simplicity, it leads to analytical results, which are in good agreement with finite element calculations. The diameters and pressures of the two bubbles can be easily varied, such that various configurations can be investigated straightforwardly. The two main results are the following:

(i) According to the mean stress distributions, the mechanical contribution to the diffusion process is likely to progressively equalize the sizes of the neighbouring bubbles.

(ii) The levels of the von Mises equivalent stresses indicate the areas where plasticity must be taken into account for a complete mechanical description of the system.

REFERENCES

1. R. LÄSSER, in "Tritium and Helium-3 in metals" (Springer Verlag, Berlin, 1989).

2. E. STERNBERG and M.A. SADOWSKY, "On the axisymmetric problem of the theory of elasticity for an infinite region containing two spherical cavities" *J. Appl. Mech.* **19** (1952) pp 19-27.

3. J. BOUSSINESQ, in "Applications des potentiels" (Gauthier-Villars, Paris, France, 1885).

4. H. MIYAMOTO, "On the problem of theory of elasticity for a region containing more than two spherical cavities" *Bulletin of JSME* **1,** 2**,** (1958) pp 103-108.

5. E. TSUCHIDA, I. NAKAHARA and M. KODAMA, "On the asymmetric problem of elasticity theory for infinite elastic solid containing some spherical cavities" *Bulletin of JSME* **19**, 135, (1976) pp 993-1000.

6. J.F. SHELLEY and Y.Y. YU, "The effect of two rigid spherical inclusions on the stresses in an infinite elastic solid" *J. Appl. Mech*. **33** (1966) pp 68-74.

7. H.S. CHEN and A. ACRIVOS, "The solution of the equations of linear elasticity for an infinite region containing spherical inclusions" *Int. J. Solids Structures* **14** (1978) pp 331-348.

8. J.R. WILLIS and R. BULLOUGH, "The interaction of finite gas bubbles in a solid" *J. Nucl. Mater*. **32** (1969) pp 76-87.

9. P.F. PAPKOVITCH, "Solution générale des équations différentielles fondamentales d'élasticité, exprimées par trois fonctions harmoniques" *C.R. Acad. Sci. Paris* **195** (1932) pp 513-515.

10. H. NEUBER, in "Kerbspannungslehre" (J.W. Edwards, Ann Arbor, Michigan, 1944).

11. J.D. ESHELBY, "The determination of the elastic field of an ellipsoidal inclusion and related problems" *Proc. Roy. Soc. London* **A241** (1957) pp 376-396.

12. T. MURA, in "Micromechanics of defects in solids" (Martinus Nijhoff Publisher, 1982).

APPENDIX

a) Analytical expressions of the A_{ij} coefficients of the linear system (17).

$$A_{11} = H(69\tau + 8)$$
$$A_{12} = H(21\tau - 8)$$
$$A_{13} = H\left\{-2\alpha_2^3\left[6\alpha_2^2(3\tau+1) + 5(3\tau-1)\right]\right\}$$
$$A_{14} = H\left\{\alpha_2^3\left[12\alpha_2^2(3\tau+1) - 5(3\tau+4)\right]\right\}$$
$$A_{21} = H\left\{-2\alpha_1^3\left[6\alpha_1^2(3\tau+1) + 5(3\tau-1)\right]\right\}$$
$$A_{22} = H\left\{\alpha_1^3\left[12\alpha_1^2(3\tau+1) - 5(3\tau+4)\right]\right\}$$
$$A_{23} = A_{11}$$
$$A_{24} = A_{12}$$
$$A_{31} = 2H\left(21\tau - 8\right)$$
$$A_{32} = 16H\left(3\tau + 1\right)$$
$$A_{33} = 2A_{14}$$
$$A_{34} = H\left\{-8\alpha_2^3\left[\left(3\alpha_2^2 - 5\right)(3\tau+1)\right]\right\}$$
$$A_{41} = 2A_{22}$$
$$A_{42} = H\left\{-8\alpha_1^3\left[\left(3\alpha_1^2 - 5\right)(3\tau+1)\right]\right\}$$
$$A_{43} = A_{31}$$
$$A_{44} = A_{32}$$

where $H = \dfrac{2\mu}{15(3\tau+4)}$ with $\tau = \dfrac{\kappa}{\mu}$

b) Analytical expressions of the eigenstrains β_{ij}.

$$\beta_{11}^{I} = -\frac{1}{12}\frac{A_{11}^{I}}{B_{11}^{I}}\frac{p}{\kappa}$$

with
$$\begin{aligned} A_{11}^{I} = {} & 20\left(81\tau^3 + 135\tau^2 + 36\tau\right)\alpha_1^5\alpha_2^6 - 8\left(486\tau^3 + 972\tau^2 + 486\tau + 72\right)\alpha_1^5\alpha_2^5 \\ & + 120\left(27\tau^3 + 63\tau^2 + 42\tau + 8\right)\alpha_1^5\alpha_2^3 - 75\left(25\tau^3 + 48\tau^2 + 16\tau\right)\alpha_1^3\alpha_2^6 \\ & + 60\left(81\tau^3 + 171\tau^2 + 96\tau + 16\right)\alpha_1^3\alpha_2^5 - 5\left(891\tau^3 + 2160\tau^2 + 1536\tau + 320\right)\alpha_1^3\alpha_2^3 \\ & + 30\left(15\tau^3 + 30\tau^2 + 16\tau\right)\alpha_2^3 + \left(243\tau^3 + 756\tau^2 + 768\tau + 256\right) \end{aligned}$$

$$\begin{aligned} B_{11}^{I} = {} & \left(225\tau^2\right)\alpha_1^6\alpha_2^6 - 144\left(9\tau^2 + 6\tau + 1\right)\alpha_1^5\alpha_2^5 + 120\left(9\tau^2 + 9\tau + 2\right)\alpha_1^5\alpha_2^3 \\ & + 120\left(9\tau^2 + 9\tau + 2\right)\alpha_1^3\alpha_2^5 - 10\left(117\tau^2 + 144\tau + 40\right)\alpha_1^3\alpha_2^3 + \left(81\tau^2 + 144\tau + 64\right) \end{aligned}$$

Similarly, $\beta_{11}^{II} = -\dfrac{1}{12}\dfrac{A_{11}^{II}}{B_{11}^{II}}\dfrac{p}{\kappa}$ where A_{11}^{II} and B_{11}^{II} are obtained from A_{11}^{I} and B_{11}^{I} by permutation of α_1 and α_2.

$$\beta^{1}_{33} = -\frac{1}{12}\frac{A^{I}_{33}}{B^{I}_{33}}\frac{p}{\kappa}$$

with
$$\begin{aligned} A^{I}_{33} &= 20\left(81\tau^3+135\tau^2+36\tau\right)\alpha_1^5\alpha_2^6 - 8\left(486\tau^3+972\tau^2+486\tau+72\right)\alpha_1^5\alpha_2^5 \\ &+120\left(27\tau^3+63\tau^2+42\tau+8\right)\alpha_1^5\alpha_2^3 - 300\left(3\tau^2+4\tau\right)\alpha_1^3\alpha_2^6 \\ &+240\left(9\tau^2+15\tau+4\right)\alpha_1^3\alpha_2^5 - 5\left(81\tau^3+540\tau^2+816\tau+320\right)\alpha_1^3\alpha_2^3 \\ &-30\left(27\tau^3+60\tau^2+32\tau\right)\alpha_2^3 + \left(243\tau^3+756\tau^2+768\tau+256\right) \end{aligned}$$

$$\begin{aligned} B^{I}_{33} &= \left(225\tau^2\right)\alpha_1^6\alpha_2^6 - 144\left(9\tau^2+6\tau+1\right)\alpha_1^5\alpha_2^5 + 120\left(9\tau^2+9\tau+2\right)\alpha_1^5\alpha_2^3 \\ &+120\left(9\tau^2+9\tau+2\right)\alpha_1^3\alpha_2^5 - 10\left(117\tau^2+144\tau+40\right)\alpha_1^3\alpha_2^3 + \left(81\tau^2+144\tau+64\right) \end{aligned}$$

Similarly, $\beta^{II}_{33} = -\frac{1}{12}\frac{A^{II}_{33}}{B^{II}_{33}}\frac{p}{\kappa}$ where A^{II}_{33} and B^{II}_{33} are obtained from A^{I}_{33} and B^{I}_{33} by permutation of α_1 and α_2.

Figure captions

Fig. 1: Decomposition of the problem.

Fig. 2: The two cavities and the set of Cartesian coordinates.

Fig. 3: The finite element mesh: (a) General view; (b) the area close to the cavities.

Fig. 4: (a) Mean stress along axis x_3 for two bubbles of same size with same pressure; (b) Mean stress along axis x_3 for two bubbles of different sizes with same pressure; (c) von Mises equivalent stress along axis x_3 for two bubbles of same size with same pressure, and (d) von Mises equivalent stress along axis x_3 for two bubbles of different sizes with same pressure.

Fig. 5: Mean stress and von Mises equivalent stress maps for two bubbles of same size with same pressure

Fig. 6: Mean stress and von Mises equivalent stress maps for two bubbles of different sizes with same pressure

Fig. 7: Von Mises equivalent stress along axis x_3 and von Mises equivalent stress maps for two bubbles of same size with different pressures

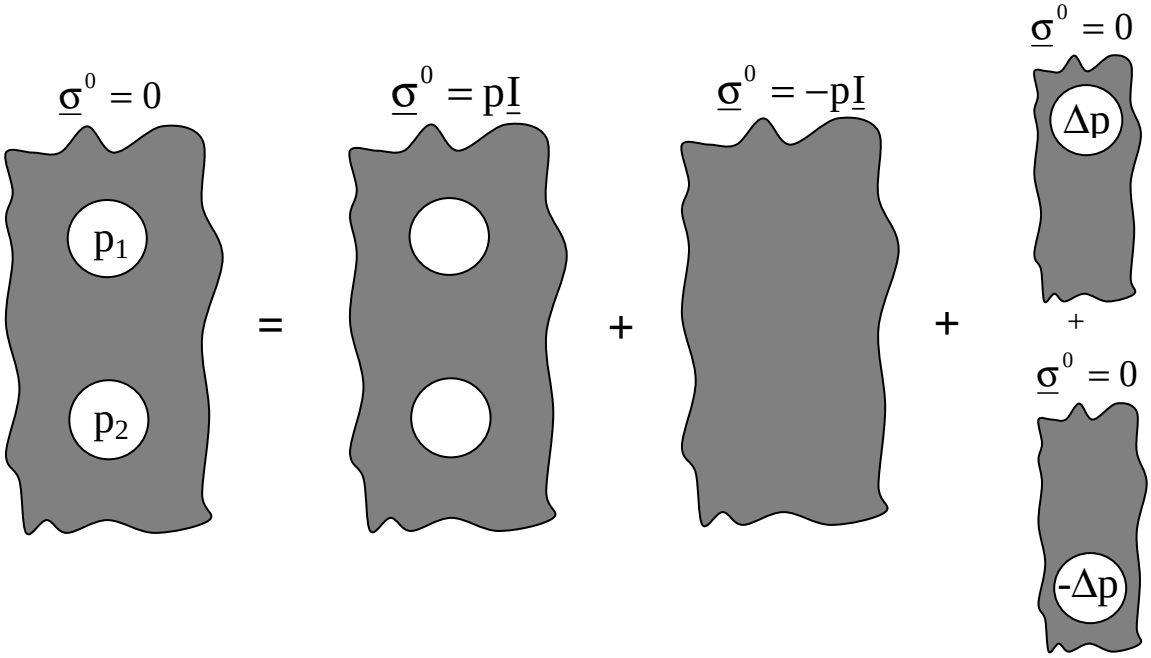

Fig. 1

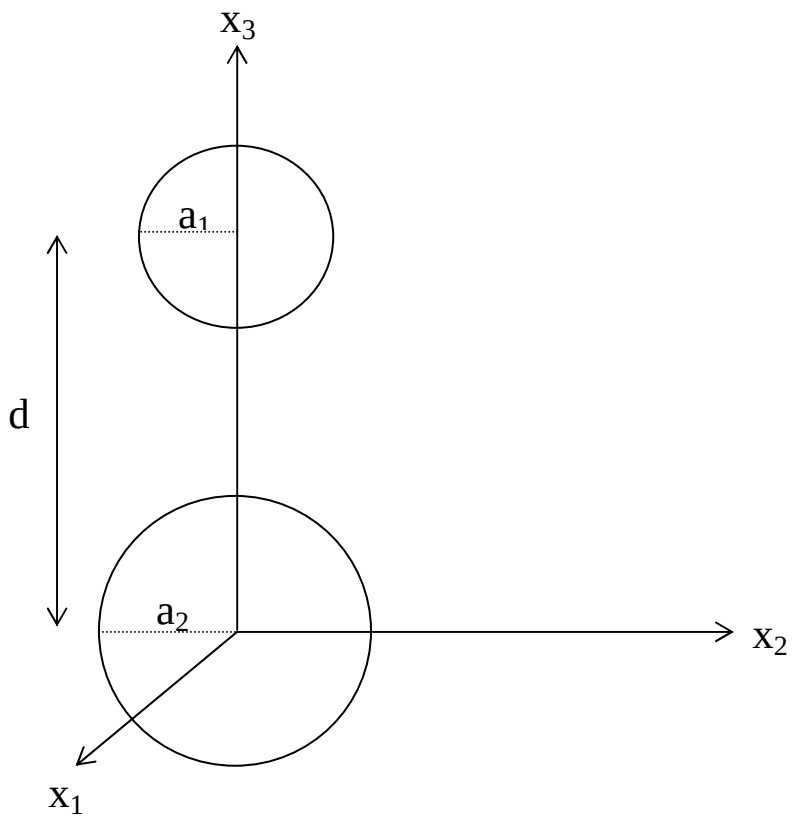

Fig. 2

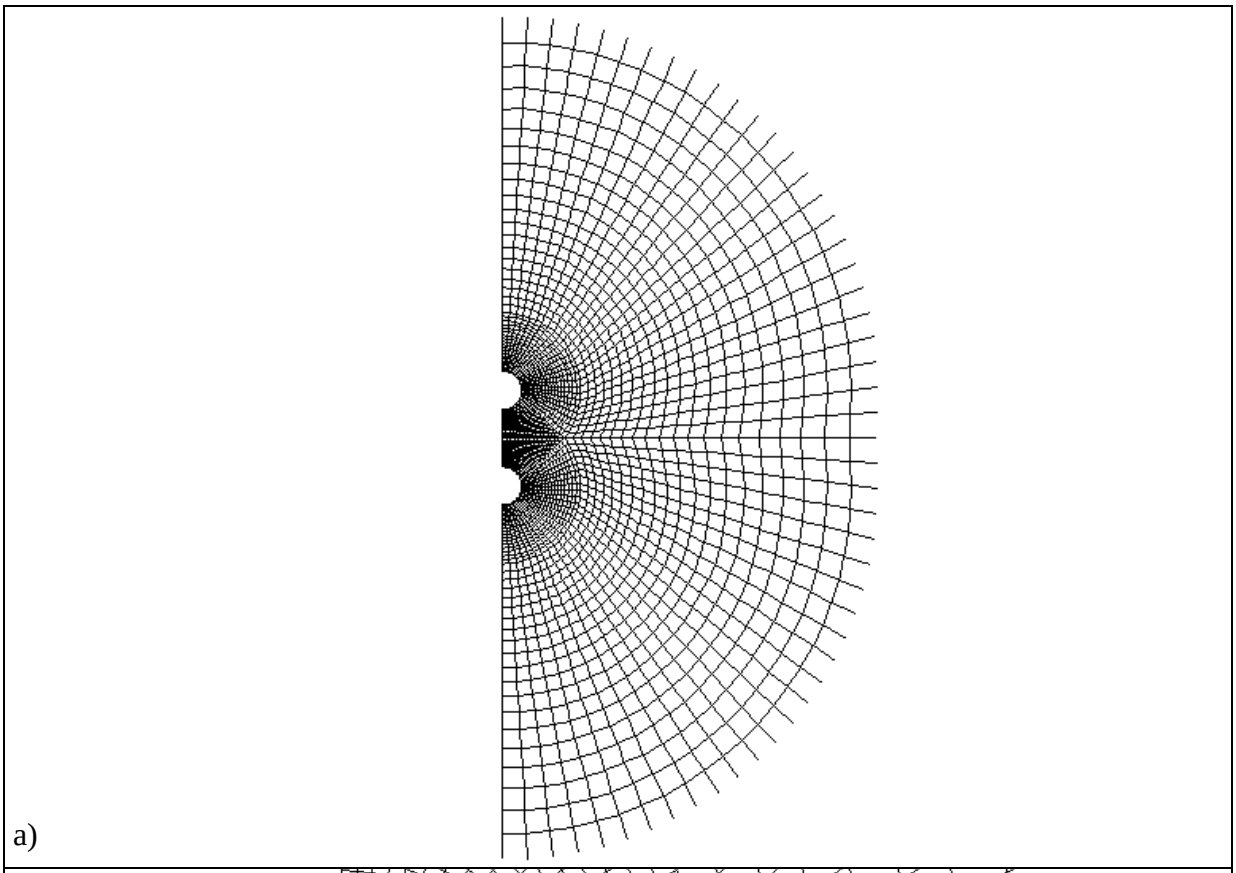

a)

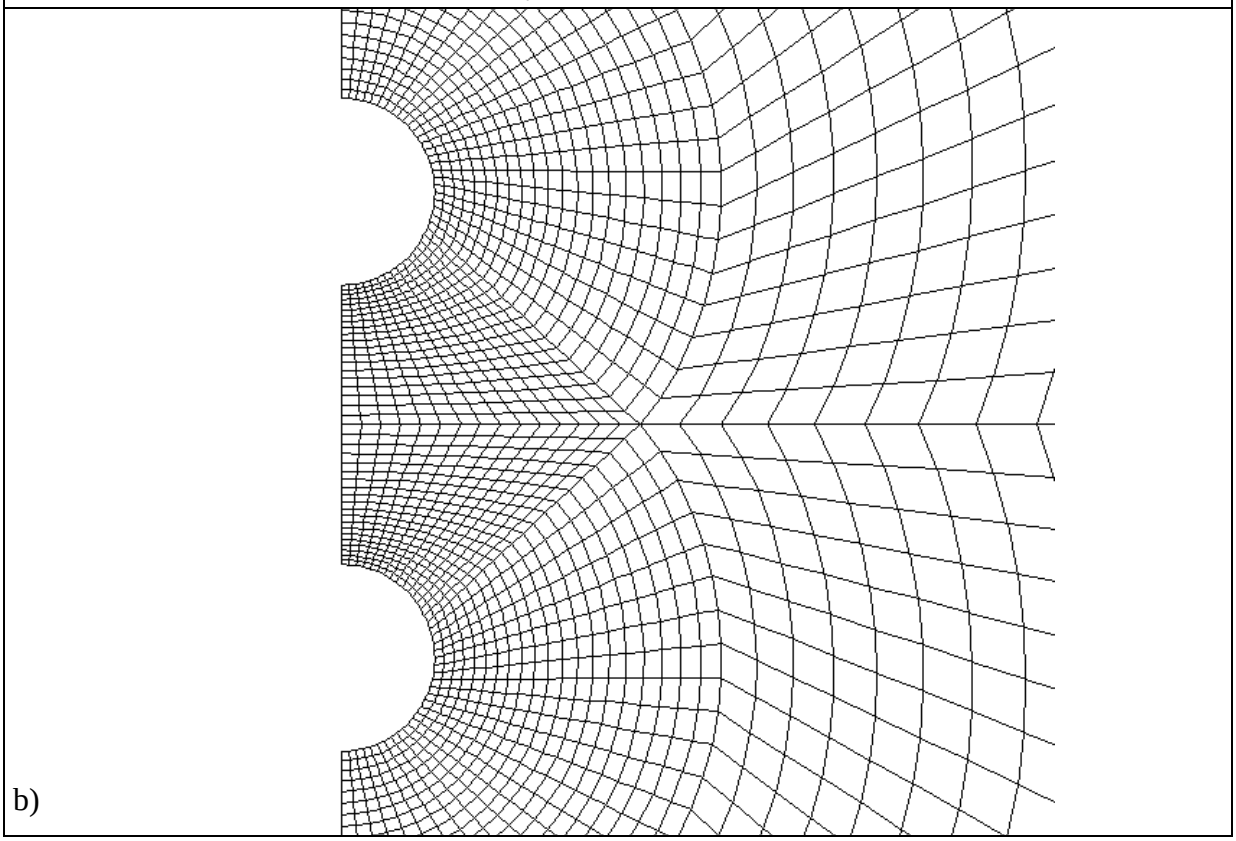

b)

Fig. 3

a=0.5nm, d=2.5nm (a/d=0.5)	a_1=0.25nm, a_2=0.75nm, d=2.5nm
mean stress along x_3, $p_1=p_2=0.5$GPa	
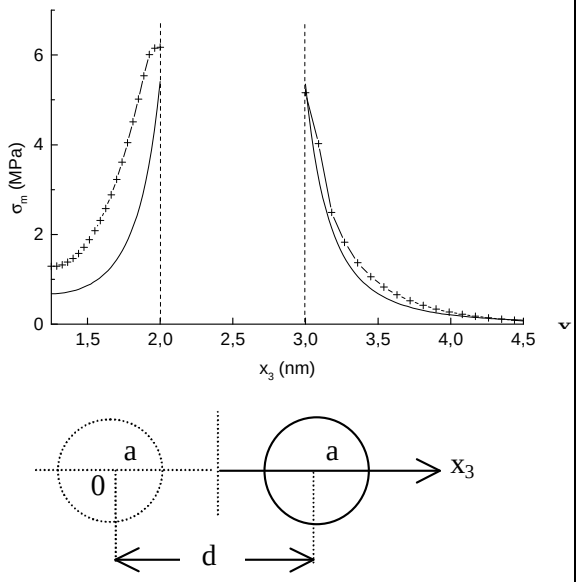 (a)	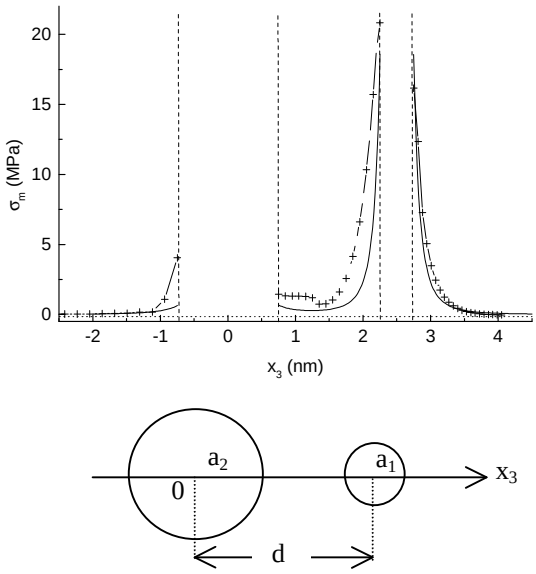 (b)
von Mises equivalent stress along x_3, $p_1=p_2=0.5$GPa	
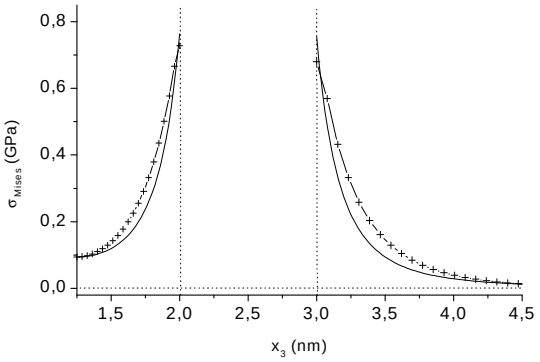 (c)	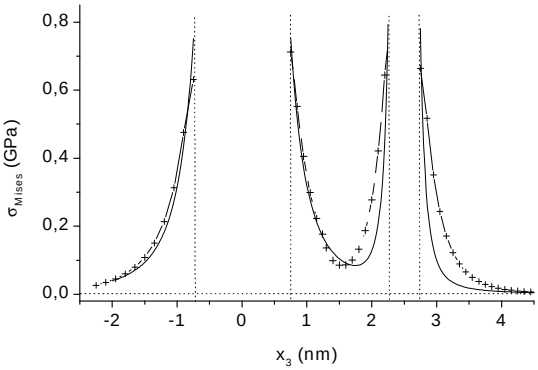 (d)
- analytical method, + numerical method	

Fig. 4

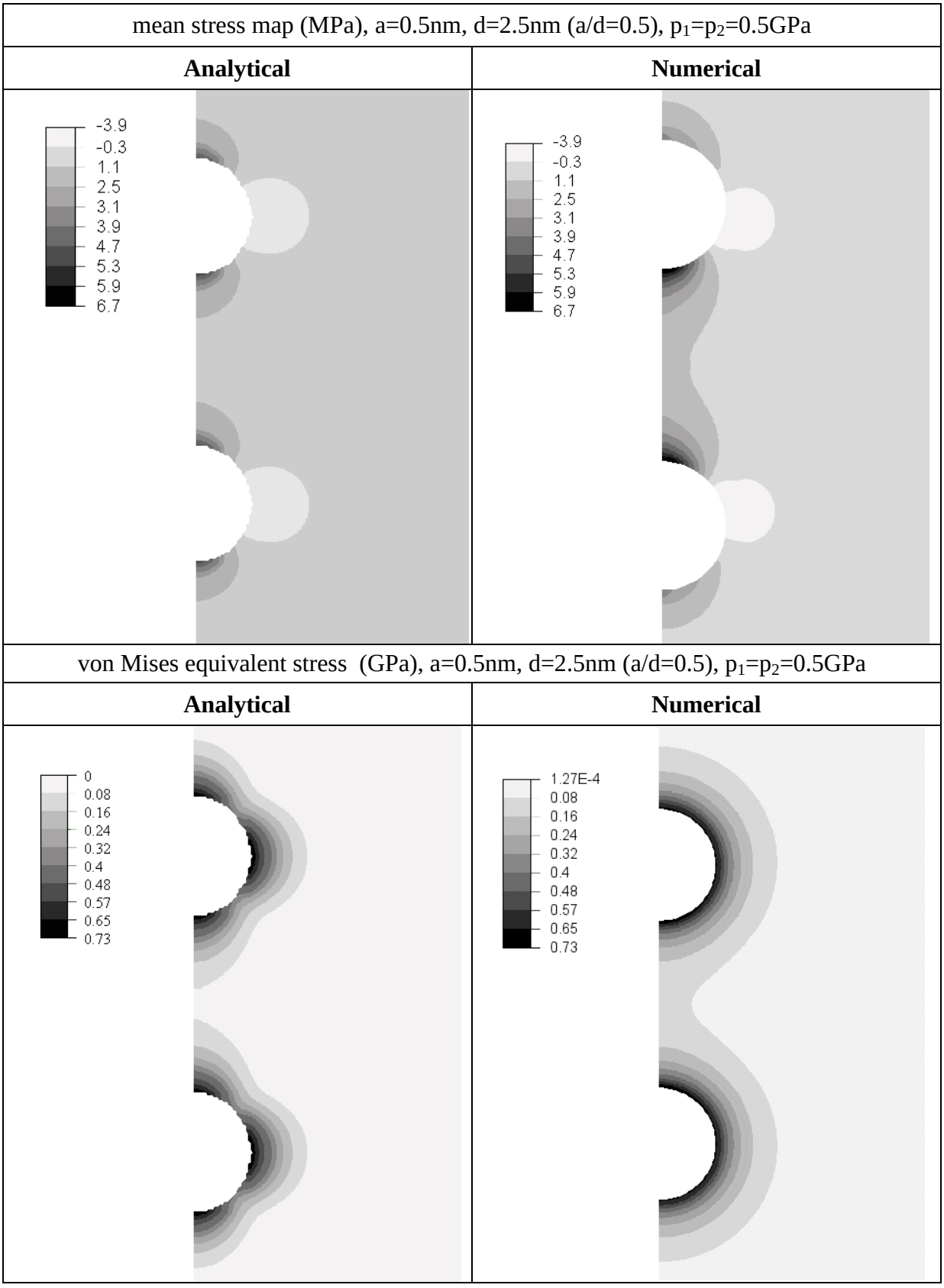
mean stress map (MPa), a=0.5nm, d=2.5nm (a/d=0.5), p1=p2=0.5GPa
Analytical
Numerical
-3.9
-0.3
1.1
2.5
3.1
3.9
4.7
5.3
5.9
6.7
von Mises equivalent stress (GPa), a=0.5nm, d=2.5nm (a/d=0.5), p1=p2=0.5GPa
Analytical
Numerical
0
0.08
0.16
0.24
0.32
0.4
0.48
0.57
0.65
0.73
1.27E-4
0.08
0.16
0.24
0.32
0.4
0.48
0.57
0.65
0.73

Fig. 5

mean stress map (MPa), a_1=0.25nm, a_2=0.75nm, d=2.5nm, p_1=p_2=0.5GPa

Analytical

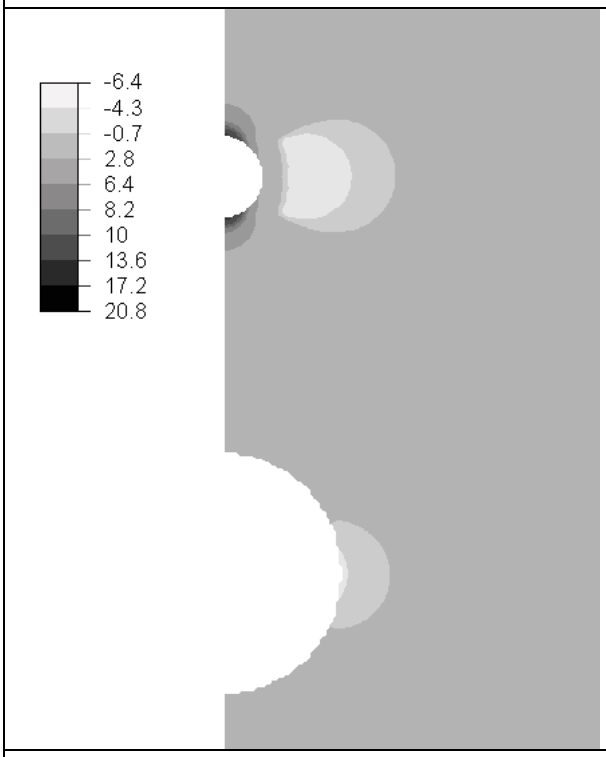

Numerical

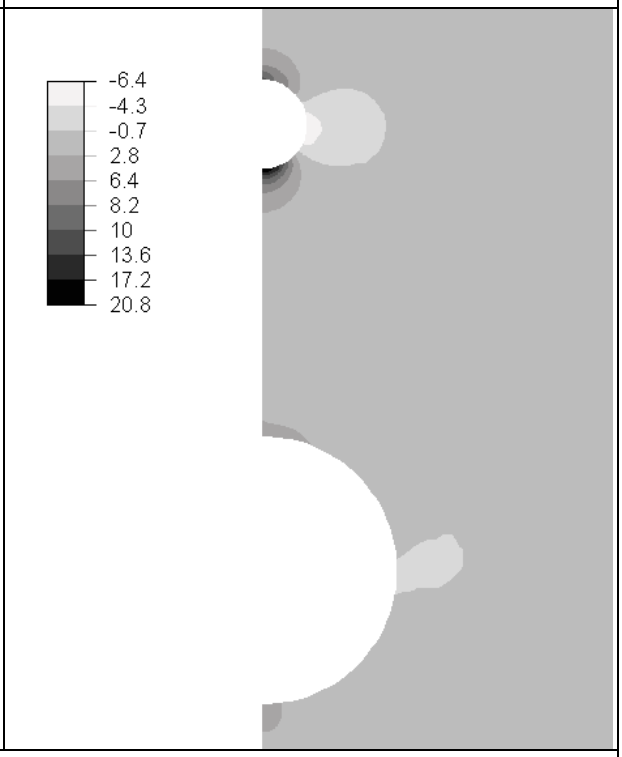

von Mises equivalent stress (GPa), a_1=0.25nm, a_2=0.75nm, d=2.5nm, p_1=p_2=0.5GPa

Analytical

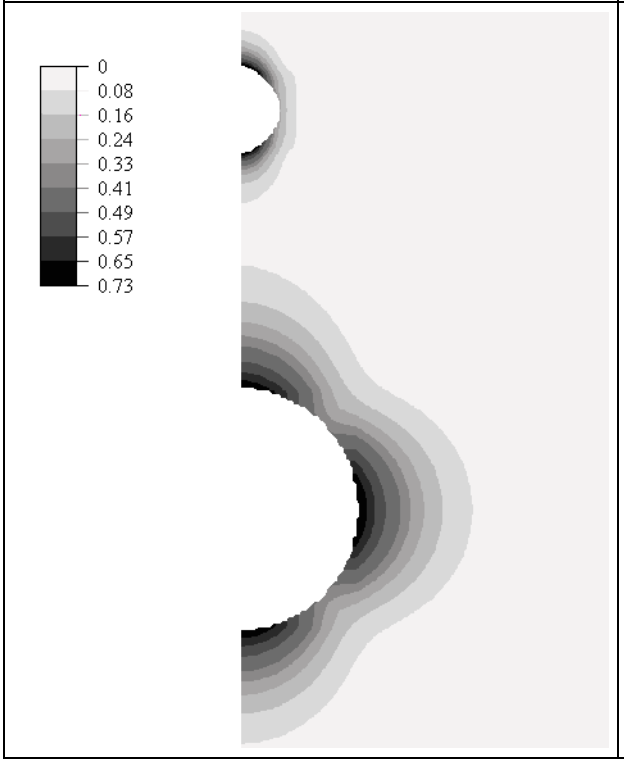

Numerical

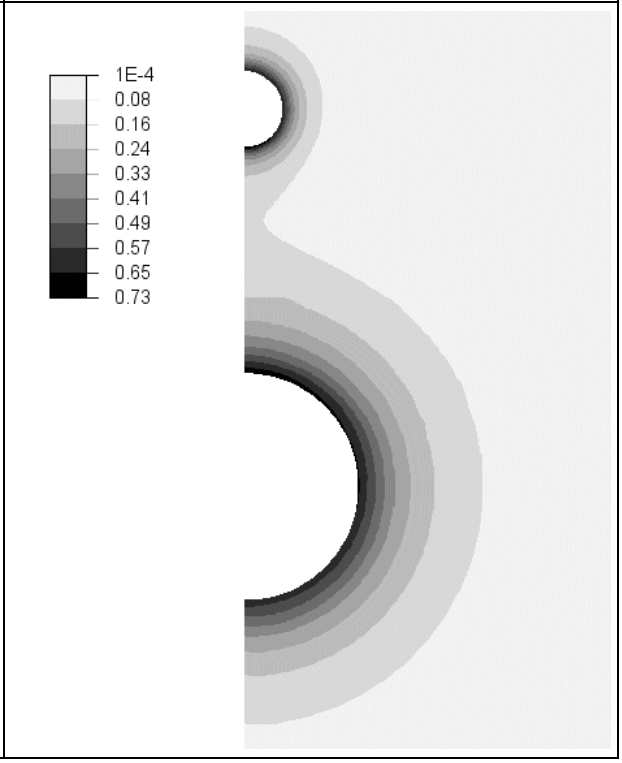

Fig. 6

von Mises equivalent stress
a=0.5nm, d=2.5nm (a/d=0.5), p1=0.6 GPa, p2=0.4 GPa
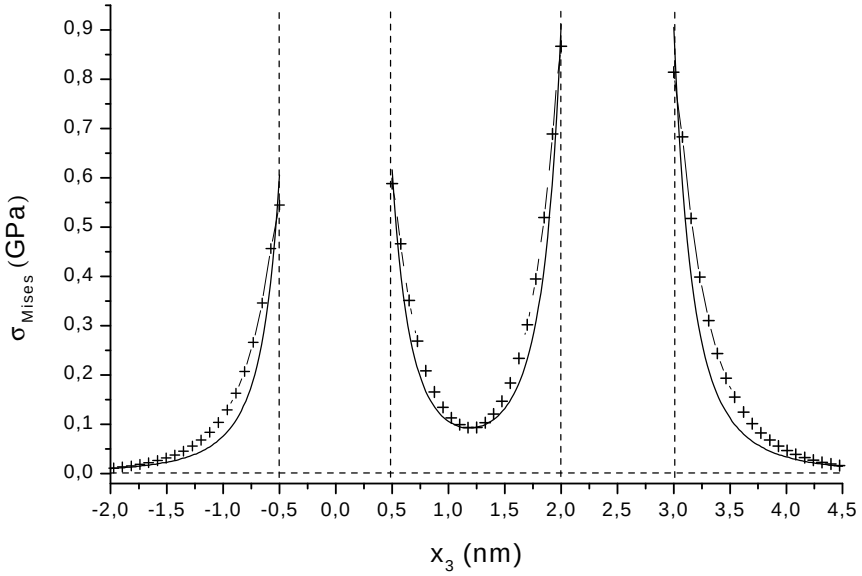 - analytical method, + numerical method
von Mises equivlent stress map (GPa)

Analytical	**Numerical**
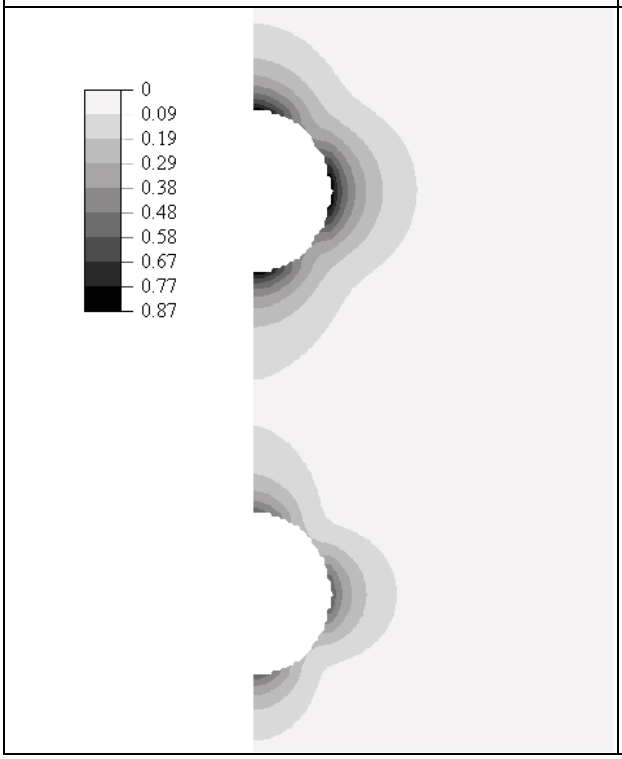	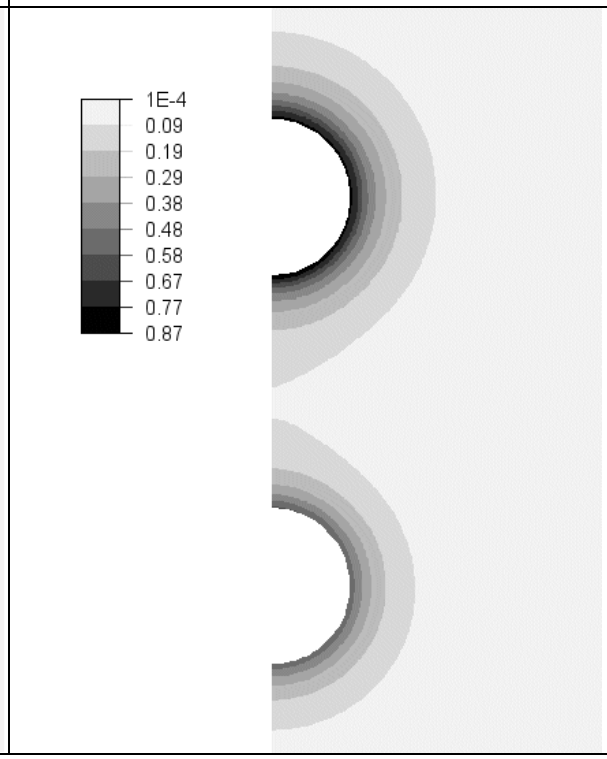

Fig. 7